Effects of 2,2',4'-trihydroxychalcone on the proliferation, metastasis and apoptosis of A549 human lung cancer cells

JIA-LIN SUN[1*], ZHAN-QI CAO[1*], SHI-WEI SUN[2], ZHONG-HUA SUN[1], SHU-HONG SUN[1], JIN-FENG YE[3] and PING LENG[1]

[1]Department of Pharmacy, The Affiliated Hospital of Qingdao University, Qingdao, Shandong 266000; [2]Department of Natural Medicine and Pharmacognosy, School of Pharmacy, Qingdao University, Qingdao, Shandong 266071; [3]School of Medicine and Pharmacy, Ocean University of China, Qingdao, Shandong 266100, P.R. China

Received October 17, 2021; Accepted January 13, 2022

DOI: 10.3892/ol.2022.13236

Abstract. The aim of the present study was to evaluate the antitumor effects of 2,2',4'-trihydroxychalcone (7a) on the A549 human lung cancer cell line. A549 cells were treated with different concentrations of 7a for different time periods. Cells without 7a were used as the negative control group. Cell proliferation, invasion, vasculogenic mimicry (VM) formation, heterogeneous adhesion and apoptosis were measured using Cell Counting Kit-8, Transwell invasion, VM, adhesion and flow cytometric assays, respectively. In addition, the expression of related proteins was determined using western blot analysis or ELISA. The present study found that 7a had a significant inhibitory effect on the survival rate of the A549 lung cancer cells but almost no effect on BEAS-2B human lung epithelial cells or human venous endothelial cells. The migration rate, VM length, invasion rate and heterogeneous adhesion number of cells treated with 7a significantly decreased as the concentration increased, while the apoptosis rate increased. Western blot analysis showed that 7a treatment significantly increased the expression levels of E-cadherin, cleaved poly (ADP-ribose) polymerase, Bax and caspase-3 and simultaneously decreased the expression levels of metalloproteinase-2/9, Bcl-2, phosphorylated (p)-PI3K, p-AKT, p-mTOR, vascular endothelial growth factor (VEGF), E-selectin and N-cadherin. At the same time, the ELISA results showed that the level of the pro-angiogenic factor VEGF in the culture media was reduced in the presence of 7a. In addition, 7a could also reduce the nuclear NF-κB protein expression, which could inhibit the gene transcription of tumor apoptosis and metastasis-related proteins. Therefore, 7a may exert inhibitory effects on A549 cells by inhibiting cell proliferation, migration, VM formation and heterogeneous adhesion, as well as by inducing apoptosis through the suppression of the PI3K/AKT/NF-κB signaling pathway; these findings suggested that 7a may be a promising agent for the treatment of lung cancer.

Correspondence to: Professor Ping Leng, Department of Pharmacy, The Affiliated Hospital of Qingdao University, 16 Jiang Su Road, Qingdao, Shandong 266000, P.R. China
E-mail: 18661808926@163.com

*Contributed equally

Key words: flavonoids, 2,2',4'-trihydroxychalcone, lung cancer, proliferation, migration

Introduction

Lung cancer can be classified into small cell lung cancer (SCLC) and non-SCLC (NSCLC). NSCLC accounts for 85% of all LC cases and can be further divided into three major pathological subtypes: Adenocarcinoma, squamous cell carcinoma and large cell carcinoma (1). Lung cancer is one of the most common types of malignant tumors in the world and a serious threat to human health and life. Lung cancer is associated with high morbidity and mortality and a poor prognosis and has a 5-year survival rate of <15%. A total of 1.8 million individuals are diagnosed with lung cancer annually, 1.6 million of which succumb to the disease (2). Early lung cancer is mainly treated by surgery, chemotherapy and radiotherapy and advanced lung cancer can be treated using molecular targeted therapy and immunotherapy. However, the 5-year survival rate is still very low and the malignant metastasis rate of lung cancer is as high as 93% (3). Therefore, adopting multitarget combination therapy, combining chemotherapy with chemobiologic therapy or exploring new target drugs could be used as an alternative lung cancer treatment.

In nature, flavonoids are widely distributed in plants and have extensive pharmacological activities, such as liver-protective, antioxidant and antitumor activities. For example, isoliquiritigenin (ISL), a flavonoid extracted from liquorice, has been confirmed to exhibit antitumor, anti-inflammatory and antioxidant effects *in vitro* and *in vivo* (4-6). In addition, ISL has been shown to have a quinone reductase activity, that can promote cancer chemoprevention (7). ISL inhibits several tumor activities, such as tumor proliferation, metastasis and apoptosis (6). In recent years, various antitumor mechanisms of ISL have been elucidated. For example, in endometrial cancer cells, ISL could induce cell cycle arrest in the G1 or G2/M phase via the p53/p21 pathway and promote apoptosis and autophagy through the activation of the extracellular

signal-regulated kinase pathway. In addition, ISL has been reported to induce cell apoptosis and inhibit proliferation via the PI3K/AKT signaling pathway (8).

2,2',4'-Trihydroxychalcone (7a) is a flavonoid and an isomer of ISL (Fig. 1). The only difference between them is that a hydroxyl group is substituted in a different place on the benzene ring. Therefore, 7a may also exhibit antitumor effects similar to those of ISL. In the present study, the effects of 7a on the proliferation, migration, invasion, vasculogenic mimicry (VM) formation, heterogeneous adhesion and apoptosis of the A549 human lung cancer cell line were first examined. At the same time, 7a had almost no effect on the proliferation of BEAS-2B human lung epithelial cells and human venous endothelial cells (HUVECs), suggesting that 7a had exhibited low cytotoxicity in normal cells. Furthermore, 7a down-regulated the expression of N-cadherin, vascular endothelial growth factor (VEGF) and metalloproteinase (MMP)-2/9, while increasing the expression of E-cadherin, Bax, caspase-3 and Bcl-2 in A549 cells. Simultaneously, 7a significantly inhibited the PI3K/AKT/NF-κB signaling pathway in A549 cells. Therefore, 7a may be a potential compound for the treatment of lung cancer.

Materials and methods

Materials. RPMI-1640 medium, DMEM, fetal bovine serum (FBS) and L-glutamine were purchased from Gibco (Thermo Fisher Scientific, Inc.). 7a and ISL were provided by the Natural Medicinal Chemistry Laboratory of Qingdao University (Shandong, China). Enhanced chemiluminescence (ECL) reagent was purchased from Beyotime Institute of Biotechnology. The subcellular structure of the cytoplasm and cell nucleoprotein extraction kit were obtained from Boster Biological Technology. Cell Counting Kit-8 (CCK-8), bovine serum albumin, Vybrant DiO cell labelling solutions, RIPA lysis buffer and PMSF were purchased from Beijing Solarbio Science & Technology Co., Ltd. Culture dishes, 6-well plates, 24-well plates and 24-well Transwell chambers with 8.0-ml polycarbonate filters were obtained from Corning, Inc. Matrigel® was purchased from BD Biosciences. An Annexin V-fluorescein isothiocyanate (FITC) apoptosis detection kit was purchased from Beyotime Institute of Biotechnology.

Cell lines. A549 human lung cancer cells, BEAS-2B human lung epithelial cells and HUVECs were obtained from the Shanghai Culture Collection of the Chinese Academy of Sciences. A549 and BEAS-2B cells were cultured in RPMI-1640 medium containing 10% FBS. HUVECs were cultured in DMEM containing 10% FBS. All media were supplemented with 100 U/ml streptomycin/penicillin. All cells were cultured in an incubator at 37˚C with 5% CO_2.

Cell proliferation assay. A cell suspension (100 μl; 1x10^3 cells/well) was inoculated in a 96-well plate. The plates were precultured in an incubator for 24 h at 37˚C with 5% CO_2. A total of 10 μl of different concentrations (0.0, 2.5, 5.0, 10.0, 20.0 and 40.0 μM) of 7a was added to the culture plate and incubated in the incubator for 24, 48 and 72 h. CCK-8 solution (10 μl) was added to each well and the plates were incubated for 1-4 h. Absorbance was measured at 450 nm using a microplate reader (Thermo Fisher Scientific, Inc). Based on the optical density values, a curve was drawn to analyze cell proliferation inhibition. The results of three independent experiments were analyzed.

Wound-healing assay. A wound-healing assay was performed in 6-well plates, as previously described by Liang *et al* (9). A549 cells were harvested and seeded on 6-well plates at a density of 4x10^5 cells in 2 ml complete RPMI-1640 medium and incubated at 37˚C for 24 h. A straight line was scrapped on the monolayer cells using a 200-μl pipette tip. Different concentrations of 7a solution were added to the cells and incubated in RPMI-1640 medium without FBS. Scratch images were then captured using a Leica DFC420 camera (Leica Microsystems, Inc.) under an inverted microscope at 0, 18 and 36 h. The gap width was analyzed along the scratch with a scale plate under an inverted microscope (Olympus Corporation; magnification, x100). At least six points were measured for each scratch. The results of three independent experiments were analyzed.

Cell invasion assay. An invasion assay was performed using 24-well Matrigel-coated Transwell chambers. Martigel was diluted 1:15 in serum-free RPMI-1640 and added into the upper chamber of Transwell chamber, and then incubated at 37˚C for 1 h. A549 cells were harvested and suspended in serum-free RPMI-1640 medium at a density of 1x10^6 cells/well. Next, 50 μl suspended cells were seeded in the upper chamber of each well and the bottom chamber was filled with 600 μl RPMI-1640 medium supplemented with 10% FBS. Following incubation at 37˚C for 24 h, cells that did not traverse the Matrigel were removed using cotton swabs. Following washing with PBS, cells that traversed the Matrigel were fixed by paraformaldehyde (4%) at room temperature for 20 min and stained with crystal violet at room temperature for 30 min. Following washing with PBS, cells that penetrated the Matrigel were counted in 10 randomly selected fields using an inverted microscope with a 20 objective (magnification, x200).

VM assay. First, Matrigel matrix glue stored at -20˚C was left to thaw at 4˚C overnight. Next, 50 μl matrix was added to a 96-well plate and placed in a cell incubator for 1 h incubation at 37˚C prior to solidification. Then, 50 μl A549 cell suspension (5x10^4/well) and 50 μl different concentrations (0.0, 2.5, 5.0 and 10.0 μM) of 7a-containing medium were added. At the same time, the solvent control group was set up. The cells were then incubated in the cell incubator for 8 h at 37˚C, and the formation of tubules was observed under a microscope and images captured. The tubule branch length was counted using ImageJ software v1.8.0 (National Institutes of Health).

ELISA. A549 cells were collected and inoculated into 24-well plates (5x10^4/well). After the cells were attached to the wall, the original medium was discarded and drug-containing media of different concentrations (0.0, 2.5, 5.0 and 10.0 μM) of 7a were added. Meanwhile, the negative control (NC) group was set up and incubation was continued in a cell incubator with 5% CO_2 for 24 h at 37˚C. The supernatant was then transferred to a centrifugal tube for centrifugation at 150 x g for 5 min at room temperature. The supernatant was then transferred to a

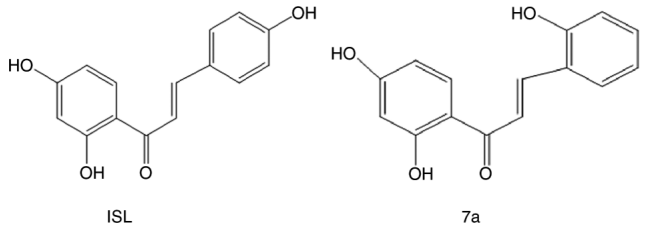

Figure 1. Chemical structure of ISL and 7a. ISL, isoliquiritigenin; 7a, 2,2',4'-trihydroxychalcone.

new centrifugal tube. The VEGF levels in each group were tested using a VEGF ELISA kit (cat. no. KE00216; Proteintech Group, Inc.), according to the manufacturer's instructions.

Cancer cell-endothelial adhesion assay. Cancer cell-endothelial adhesion was performed as previously described (10). A549 cells were cultured in 6-well plates with different concentrations (0.0, 2.5, 5.0 and 10.0 μM) of 7a and HUVECs were cultured in 24-well plates. Following incubation at 37˚C for 48 h, A549 cells were washed with PBS and labelled using 5 μM DiO fluorescent cell labelling solution in serum-free RPMI-1640 medium for 30 min at 37˚C. Next, tumor cells were washed with PBS and removed from the culture plates. A549 cells were collected using centrifugation at 150 x g for 3 min at room temperature. Following washing, $5x10^4$ cells were applied to the HUVEC monolayer cultured in 24-well plates for 1 h at 37˚C. Next, the 24-well plates were gently washed with PBS and the fluorescently labelled cells were counted in 10 randomly selected fields using an Olympus B51 fluorescence microscope (Olympus Corporation) with a 10 objective (magnification, x100).

Cell apoptosis analysis. A549 cells were either treated with different concentrations (0, 5, 10 and 20 μM) of 7a or 0.1% DMSO for 48 h at 37˚C. The cell suspension (~$10x10^4$) was collected and centrifuged at 150 x g for 5 min at room temperature. The supernatant was discarded and the cells were gently resuspended in 195 μl Annexin V-FITC binding solution. Annexin V-FITC (5 μl) was added to the cells and mixed gently. Propidium iodide (PI) staining solution (5 μl) was added and mixed gently. The cells were incubated in the dark for 10-20 min at room temperature and then placed in an ice bath. Early + late apoptotic cells were then detected via flow cytometer (FACSVantage; BD Biosciences) using the apoptosis detection kit, following the manufacturer's instructions. Annexin V-FITC fluorescence was green and PI fluorescence was red. The flow cytometry results were analyzed using FlowJo software v7.6.5 (FlowJo LLC). The results were analyzed from three independent experiments.

Western blot analysis. A549 cells were seeded in 6-well plates ($2x10^5$ cells per well). A total of 24 h later, the cells were treated with different concentrations (0.0, 2.5, 5.0 and 10.0 μM) of 7a. Following incubation at 37˚C for 48 h, cell lysates were collected in RIPA lysis buffer PMSF (99:1, v/v) and centrifuged at 15,000 x g for 15 min at 4˚C. The total protein concentrations were then determined using a Pierce BCA Protein Assay kit (Thermo Fisher Scientific, Inc.). Adequate buffer (6X) was added to the total protein and mixed completely. The mixture was then heated at 100˚C for 5 min. Next, 15-30 μg total protein was fractionated using 10% sodium dodecyl sulphate-polyacrylamide gel electrophoresis and transferred to polyvinylidene fluoride membranes (MilliporeSigma). The membranes were blocked with 5% non-fat milk at room temperature for 4 h, and then cultured overnight at 4˚C with the following primary antibodies: E-cadherin (1:1,000; cat. no. 14472s; mouse monoclonal), N-cadherin (1:1,000; cat. no. 4061s; rabbit monoclonal), MMP-9 (dilution, 1:1,000; cat. no. 13667Ts; rabbit monoclonal), MMP-2 (dilution, 1:1,000; cat. no. 4022s; rabbit polyclonal), VEGF (dilution, 1:1,000; cat. no. 65373s; rabbit polyclonal), E-Selectin (1:1,000; cat. no. 20894-1-AP; rabbit polyclonal), Bcl-2 (1:1,000; cat. no. 15071s; mouse monoclonal), Bax (1:1,000; cat. no. 5023s; mouse monoclonal), Cleaved-PARP (dilution, 1:1,000; cat. no. 5625s; rabbit monoclonal), Caspase-3 (dilution, 1:1,000; cat. no. 9662s; rabbit polyclonal), PI3K (dilution, 1:1,000; cat. no. 4249s; rabbit monoclonal), p-PI3K (dilution, 1:1,000; cat. no. 17366s; rabbit monoclonal), AKT (dilution, 1:1,000; cat. no. 9272s; rabbit polyclonal), p-AKT (dilution, 1:1,000; cat. no. 4060s; rabbit monoclonal), mTOR (dilution, 1:1,000; cat. no. 2972s; rabbit polyclonal), p-mTOR (dilution, 1:1,000; cat. no. 5536s; rabbit monoclonal), PCNA (dilution, 1:1,000; cat. no. 13110T; rabbit monoclonal) and β-actin (dilution, 1:1,000; cat. no. 4970s; rabbit monoclonal). Primary E-Selectin antibody was from ProteinTech Group, Inc. Other primary antibodies were from Cell Signaling Technology, Inc. According to the sources of the different primary antibodies, the membranes were incubated with horseradish peroxidase conjugated goat anti-rabbit or goat anti-mouse IgG secondary antibodies (cat. nos. SA00001-2 and SA00001-1, respectively; dilution, 1:10,000; ProteinTech Group, Inc.) at room temperature for 1 h and then laid on the developer board of the gel image processing instrument. ECL (Beyotime Institute of Biotechnology) was added to allow visualization of the signals. Image Lab software v3.0 (Bio-Rad Laboratories, Inc.) was used for band processing and analysis and β-actin was used as an internal reference for semi-quantitative analysis of protein expression in each group.

Reverse transcription-quantitative PCR (RT-qPCR) analysis. A549 cells were seeded in 6-well plates ($2x10^5$ cells per well) and incubated at 37˚C for 24 h. The cells were treated with different concentrations (0, 2.5, 5 and 10 μM) of 7a and incubated at 37˚C for 48 h. Total RNA was extracted from the 6-well plates using TRIzol® reagent (Thermo Fisher Scientific, Inc.). The RNA concentration was determined by measuring ultraviolet absorption at 260 and 280 nm. The A260/A280 ratio was calculated to assess RNA quality and purity. Next, 1 mg RNA was reverse-transcribed using a PrimeScript RT reagent kit (Takara Bio, Inc.). cDNA was diluted (2 μl) and selectively amplified using a PCR with SYBR Green I (Takara Bio, Inc.) and specific primers. Primers were designed by Shanghai Bioengineering, as follows: NF-κB, forward 5'-GCT GCATCCACAGTTTCCAG-3', reverse 5'-TCCCCACGCTGC TCTTCTAT-3'; GAPDH, forward 5'-AATGGGCAGCCGTTA GGAAA-3', reverse 5'-GCCCAATACGACCAAATCAGA G-3'. The samples were amplified using a Roche LightCycler 480II (Roche Diagnostics). All procedures were performed

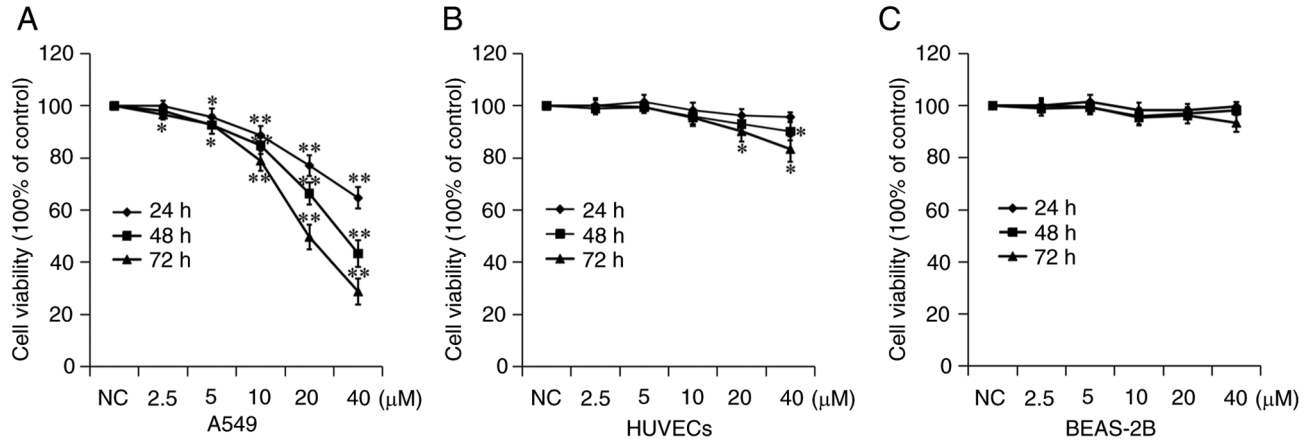

Figure 2. Inhibitory effects of 7a on the proliferation of (A) A549, (B) HUVECs and (C) BEAS-2B cells were measured using a CCK-8 assay following incubation with various concentrations of 7a for 24, 48 and 72 h. Data are presented as the mean ± standard deviation of three separate experiments. *P<0.05 and **P<0.01 vs. NC. 7a, 2,2',4'-trihydroxychalcone; NC, negative control; HUVEC, human venous endothelial cell.

according to the manufacturer's protocols. The relative quantity of NF-κB mRNA was calculated using a comparative method ($2^{-\Delta\Delta Cq}$) against a GAPDH endogenous control (n=3) (11).

Statistical analysis. All experiments were repeated three times. SPSS software 22.0 (IBM Corp.) was used for the statistical analysis of all data and the experimental results were expressed as the mean ± standard deviation. The difference between the groups was analysed using one-way ANOVA. Tukey's post hoc test was performed after one-way ANOVA. P<0.05 was considered to indicate a statistically significant difference.

Results

7a inhibits A549 cell proliferation. The inhibitory effect of 7a on the proliferation of A549 cells was measured using a CCK-8 assay. A549 cells were treated with different concentrations of 7a for 24, 48 and 72 h. The viability of A549 cells was determined and the growth curves of A549 cells were drawn. As shown in Fig. 2, 7a inhibited the proliferation and growth of A549 cells in a time- and dose-dependent manner. The IC_{50} value of 7a against A549 cells was calculated (Fig. 2A). The results showed that the IC_{50} of 7a on A549 cell growth was 65.72±4.20, 33.46±4.11 and 19.86±2.33 μM at 24, 48 and 72 h, respectively. These results indicated that 7a could inhibit the proliferation of A549 cells at higher concentrations and for longer durations.

The toxic effects of 7a were examined on two types of normal human tissue cells. Normal BEAS-2B human lung epithelial cells and HUVECs were selected. The CCK-8 test results showed that 7a had no significant inhibitory effect on the proliferation of these two types of cells. Among them, although HUVECs were relatively sensitive to 7a, the maximum proliferation inhibition rate was <20% at 40 μM and 72 h. These results indicated that 7a had a selective tumor cell-killing effect, but had no obvious toxicity or side effects on normal cells, suggesting its clinical application potential.

7a inhibits A549 cell migration and invasion. According to the results of the CCK-8 experiment, 2.5 and 5 μM were selected as the low cytotoxic drug concentrations for the migration and invasion experiments. First, the effect of 7a on the migratory ability of A549 cells was tested using a cell scratch assay and the results showed that 7a could significantly inhibit the migratory ability of A549 cells. The migration rate of NC, 2.5 and 5 μM group was respectively ~43.61, 21.30 and 17.52% at 18 h and 61.50, 31.22 and 22.10% at 36 h (Fig. 3A). The effect of 7a on the invasive ability of A549 cells was also examined, using a Transwell invasion assay. As compared with the NC group, the number of A549 cells passing through the compartment was reduced in the 7a group at 48 h, especially in the high-concentration (5 μM) group (Fig. 3B). These results demonstrated that 7a could markedly inhibit the migration and invasion of A549 cells at non-cytotoxic concentrations.

To understand the mechanism through which 7a inhibits the migration and invasion of A549 cells, the expression of cell metastasis-related proteins was further investigated. As shown in Fig. 3C, 7a could significantly increase the expression of E-cadherin while at the same time decreasing the expression of MMP-9 and -2 suggesting that the 7a-induced inhibition of migration and invasion may be due to the regulation of the expression of these proteins.

7a inhibits VM. Highly invasive tumor cells, such as NSCLC, can form mimicry vessels; that is, tumor cells exhibit certain characteristics that are similar to vascular endothelial cells and can degrade the basement membrane to connect and form a network structure (12,13). Therefore, in the *in vitro* mimicry angiogenesis experiments, Matrigel was used to simulate the basement membrane and the simulated angiogenesis of tumor cells in each group observed. In the NC group, A549 cells were connected to form multiple grid structures (Fig. 4A). However, in the 7a dosage group, the branch length of mimetic vessels was significantly reduced, particularly following treatment with 10 μM 7a for 8 h. The cells were dispersed, almost no tubules were formed and the inhibition rate of mimetic vessel formation was as high as 82.89%. These results indicated that 7a could significantly inhibit the formation of mimicry vessels in A549 cells in a concentration-dependent manner.

As a proangiogenic factor, VEGF not only serves an important role in angiogenesis but is also associated with

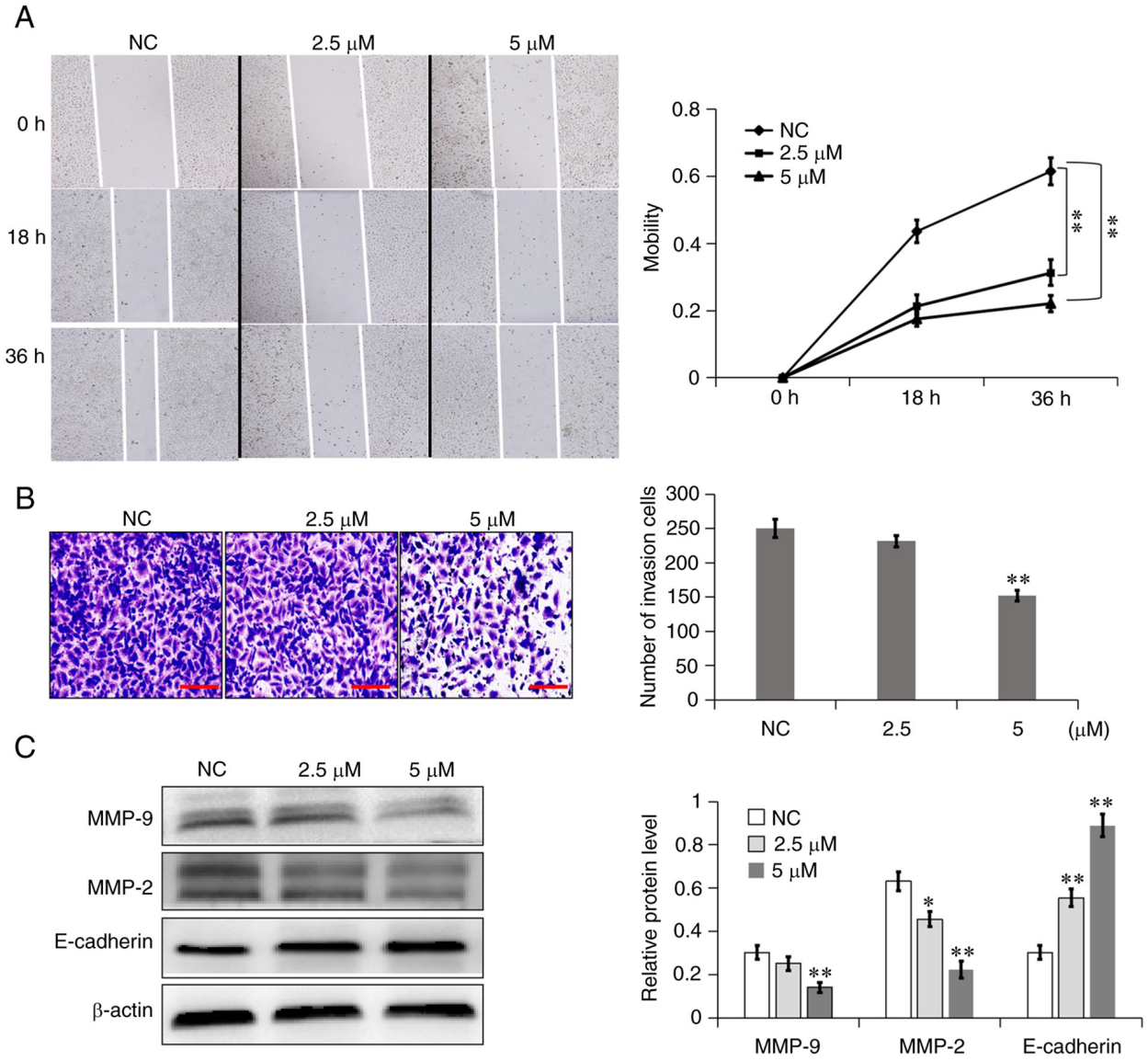

Figure 3. Noncytotoxic effects of 7a on the migration and invasion of A549 cells following treatment with different 7a concentrations. (A) A wound-healing assay was performed to detect the migration of A549 cells following treatment with 7a for 0, 18 and 36 h. (B) A549 cells treated with different concentrations of 7a were placed on filters with Matrigel and incubated for 24 h (scale bar=50 μm). (C) The expression of MMP-2/9 and E-cadherin in A549 cells following treatment with different concentrations of 7a for 24 h was measured using western blot analysis. Data are presented as the mean ± SD from three independent experiments. *P<0.05 and **P<0.01 vs. NC. 7a, 2,2',4'-trihydroxychalcone; NC, negative control; MMP, metalloproteinase.

tumor cells (14). Western blot analysis and ELISA were used to determine the effect of 7a on the expression and secretion of VEGF in A549 cells and culture media. As shown in Fig. 4B, 7a inhibited the expression of VEGF in A549 cells compared with the NC group. ELISA results (Fig. 4C) showed that in A549 cells treated with different concentrations of 7a for 24 h, VEGF secretion was significantly reduced in a concentration-dependent manner. The results suggested that 7a could significantly inhibit the expression and secretion of VEGF in 549 cells.

7a inhibits A549 cell adhesion to HUVECs. The heterogeneous adhesion of tumor cells is a pivotal step in tumor metastasis. A549 cells treated with different concentrations of 7a were stained with DiO dye and then added to 24-well plates covered with a single layer of HUVECs, which could mimic the adhesion of tumor cells to the lining of blood vessels. The adhesion of A549 cells to HUVECs was examined following incubation with different concentrations of 7a for 48 h. The fluorescent cells above the HUVEC monolayer were A549 cells. The results showed that 2.5, 5 and 10 μM 7a significantly reduced A549 cell adhesion to HUVECs by 3.12, 13.8 and 34.4%, respectively (Fig. 5A). The results suggested that 7a could inhibit the adhesion of A549 cells to HUVECs in a concentration-dependent manner.

Next, the molecular mechanism through which 7a regulates the adhesion of A549 cells to vascular endothelial cells was explored. The relevant adhesion protein levels were detected using western blot analysis. As shown in Fig. 5B, the expression of N-cadherin and E-selectin was significantly reduced following treatment with different concentrations of 7a. These two adhesion molecules have been proven to be involved in adhesion between tumor cells and HUVECs (10,15). Adhesion could then promote tumor cell aggregation in the blood vessels,

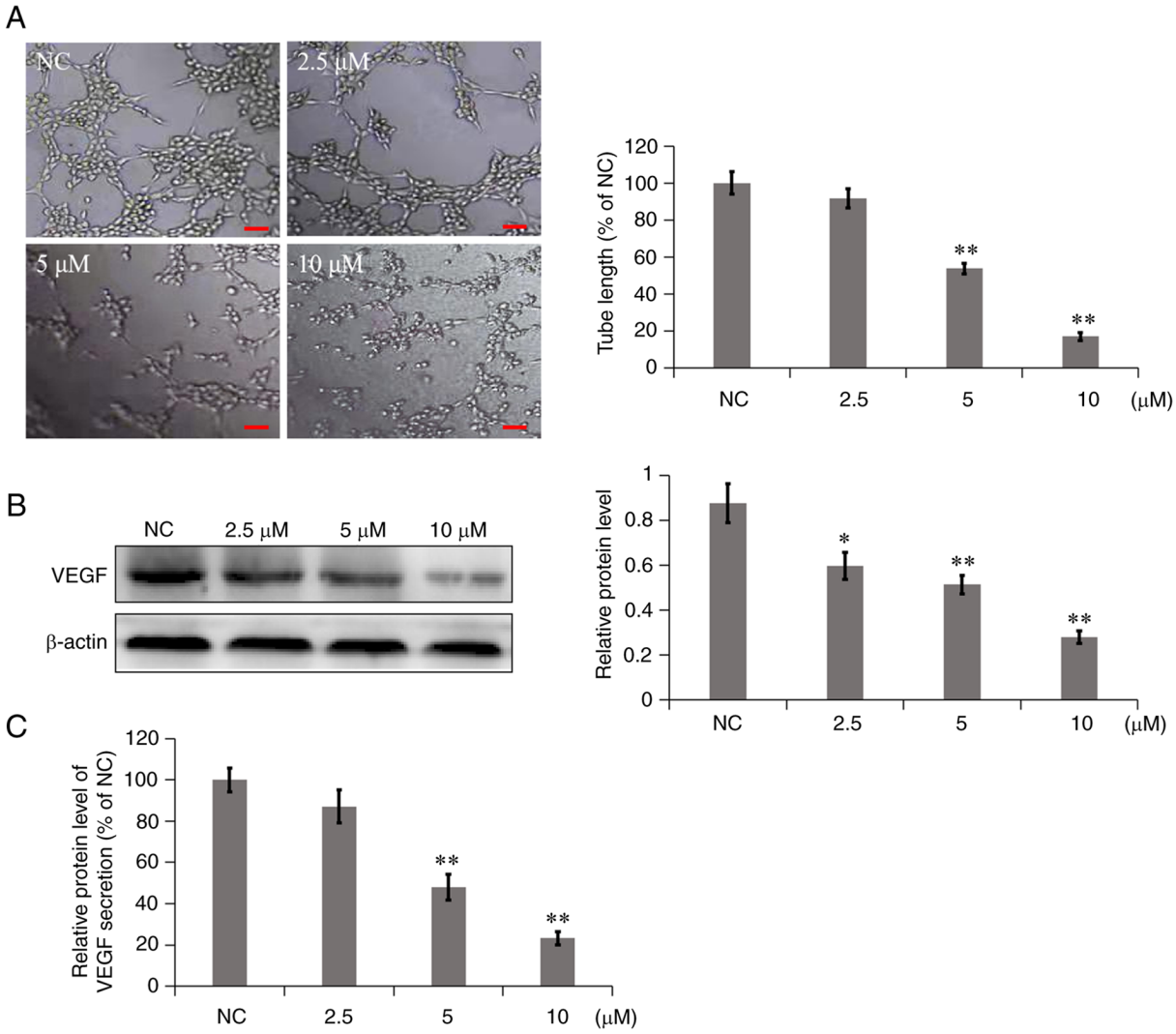

Figure 4. Inhibitory effect of 7a on the VM formation of A549 cells. (A) 7a suppressed VM formation in A549 cells *in vitro*. Representative images of VM formation following treatment with different concentrations of 7a for 8 h (bar=200 μm). (B) 7a inhibited the expression of VEGF in A549 cells *in vitro*. The cellular expression of VEGF in A549 cells following treatment with different concentrations of 7a for 24 h was measured using western blot analysis. (C) The secretion of VEGF in A549 cell culture medium treated with 7a for 24 h was examined using ELISA. Data are presented as the mean ± SD from three independent experiments. *P<0.05 and **P<0.01 vs. NC group. NC, negative control. 7a, 2,2',4'-trihydroxychalcone; VM, vasculogenic mimicry; VEGF, vascular endothelial growth factor.

which could avoid anoikis and increase the tumor metastasis potential. Therefore, 7a may inhibit A549 cell metastasis by inhibiting the expression of N-cadherin and E-selectin.

7a promotes A549 cell apoptosis. The effects of different concentrations of 7a on the apoptosis of A549 cells were quantitatively determined via Annexin V-FITC/PI double staining. Normal live, early apoptotic, necrotic and late apoptotic cells could be distinguished by using flow cytometry. As shown in Fig. 6A, the apoptosis rate of A549 cells in the NC group was 5.4%. The total apoptotic rate of A549 cells increased to 9.6, 16 and 28.2% following treatment with 5, 10 and 20 μM 7a for 48 h, respectively. To further explore the mechanism through which 7a induces A549 cell apoptosis, the effect of 7a on the expression of mitochondrial apoptosis-related proteins was detected via western blot analysis. As shown in Fig. 6B, the expression levels of the proapoptotic proteins Bax, cleaved poly (ADP-ribose) polymerase (PARP) and caspase-3 were significantly increased, while the expression of the antiapoptotic protein Bcl-2 was significantly decreased. This result indicated that the promotion of A549 cell apoptosis by 7a may be associated with the mitochondrial apoptosis pathway.

7a inhibits the activation of the PI3K/AKT signaling pathway. A wide range of biological processes in a variety of tumor cells is regulated by the PI3K/AKT signaling pathway, including cell proliferation, apoptosis, survival, growth and movement. The AKT and mTOR proteins have been reported to serve an important role in tumor cell viability and metastasis (16). In the present study, the aforementioned proteins were investigated in the PI3K/AKT signaling pathway using western blot analysis. As shown in Fig. 7, the phosphorylation levels of PI3K, AKT and mTOR in the 7a dosage group were significantly decreased in A549 cells. In addition, the NF-κB level was examined in the cytoplasm and nucleus. As shown in Fig. 8A, NF-κB levels in the cytoplasm of the 7a dosage group were slightly decreased, while NF-κB levels in the nucleus were markedly

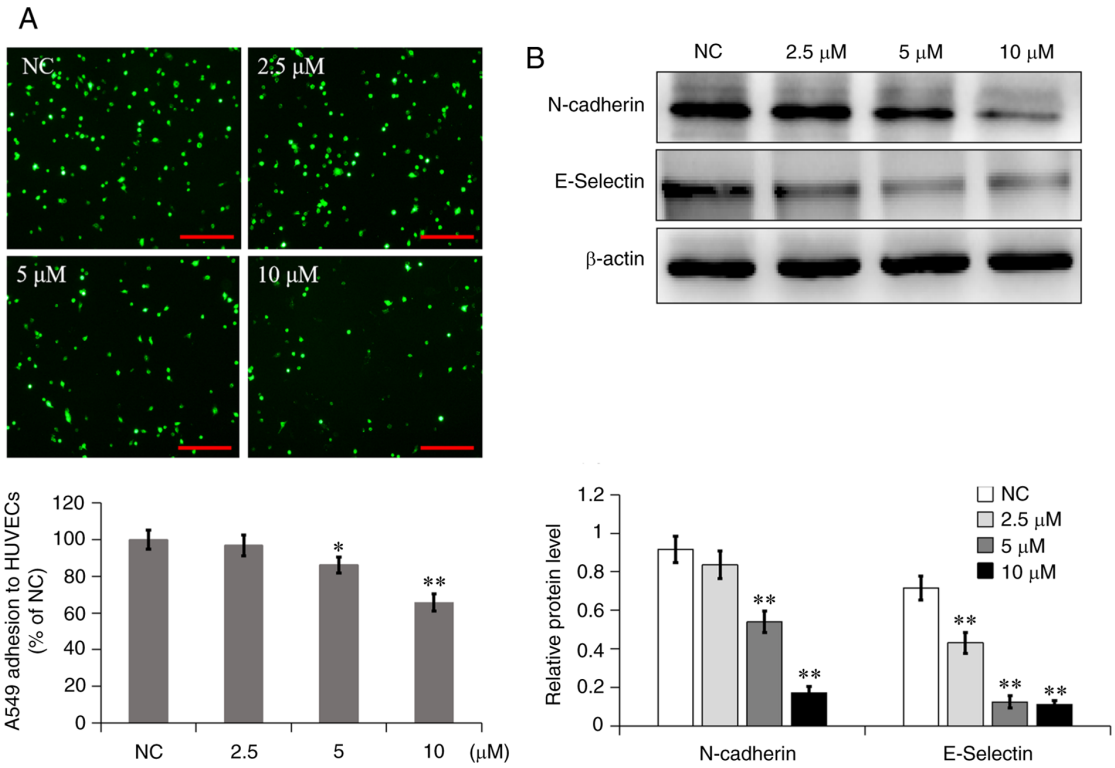

Figure 5. Inhibitory effect of 7a on A549 cell adhesion to HUVEC monolayers. (A) The fluorescently labelled cells were counted in 5 and 10 randomly selected low-power fields under a fluorescence microscope (bar=100 μm). (B) The expression of N-cadherin and E-selectin in A549 cells following 7a treatment for 48 h was determined using western blot analysis. Data are presented as the mean ± SD from three independent experiments. *P<0.05 and **P<0.01 vs. NC. 7a, 2,2',4'-trihydroxychalcone; HUVEC, human venous endothelial cell; NC, negative control.

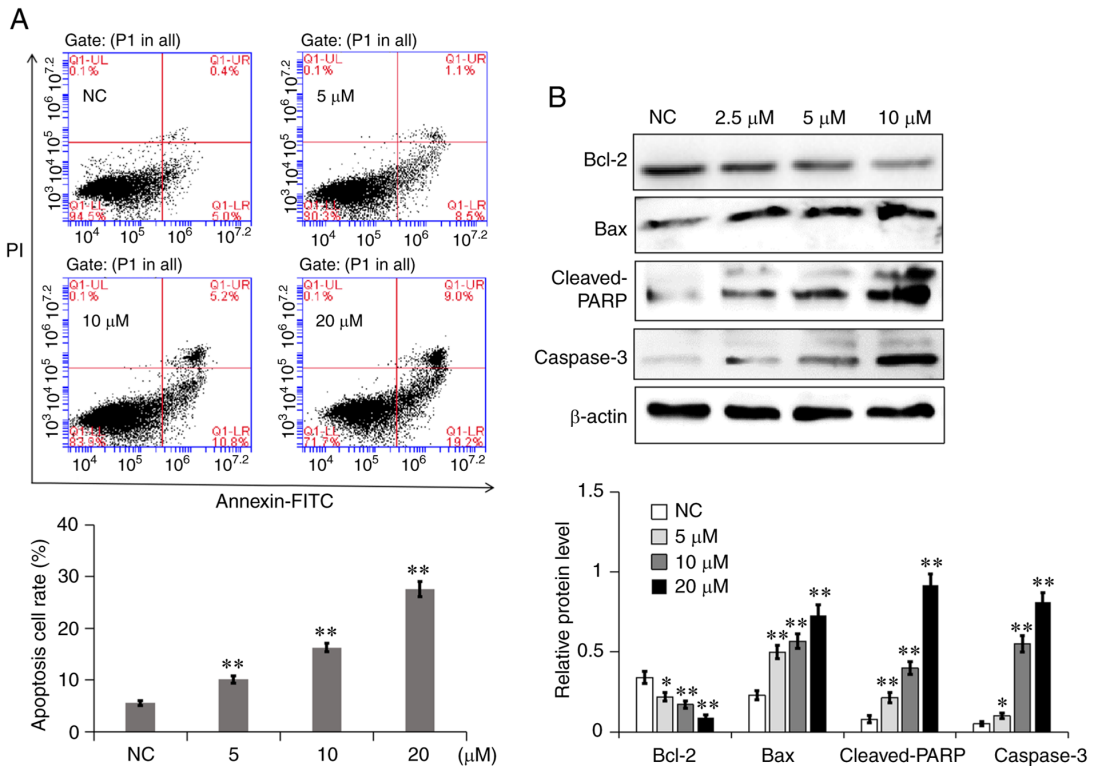

Figure 6. 7a induces A549 cell apoptosis through the mitochondrial apoptosis pathway. (A) Detection of apoptotic A549 cells after Annexin V/PI using flow cytometry, following their treatment with different concentrations of 7a for 48 h. LL, LR, UR and UL represent normal, early apoptotic, late apoptotic and necrotic cells, respectively. The percentage of apoptotic cells (both early and late) was scored in three separate experiments. (B) The expression of four apoptosis-related proteins in A549 cells following 7a treatment for 48 h was measured using western blot analysis. The semiquantitative expression levels of the proteins were measured using exposure grey value. Data are presented as the mean ± SD from three independent experiments. *P<0.05 and **P<0.01 vs. NC. 7a, 2,2',4'-trihydroxychalcone; NC, negative control; LL, Lower left; LR, Lower right; UR, Upper right; UL, Upper left; PARP, poly (ADP-ribose) polymerase.

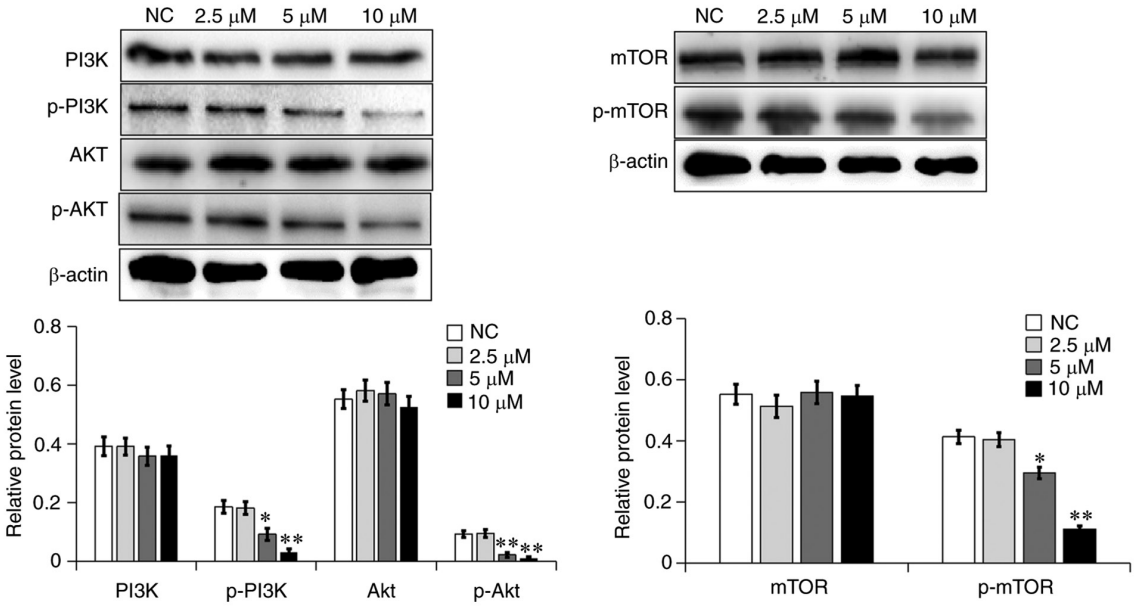

Figure 7. 7a inhibits the activation of the PI3K/AKT signaling pathway in A549 cells. The effects of 7a on the expression of PI3K, p-PI3K, AKT, p-AKT, mTOR and p-mTOR in A549 cells were detected by western blot analysis. Data are presented as the mean ± SD from three independent experiments. *P<0.05 and **P<0.01 vs. NC. 7a, 2,2',4'-trihydroxychalcone; NC, negative control; p-, phosphorylated.

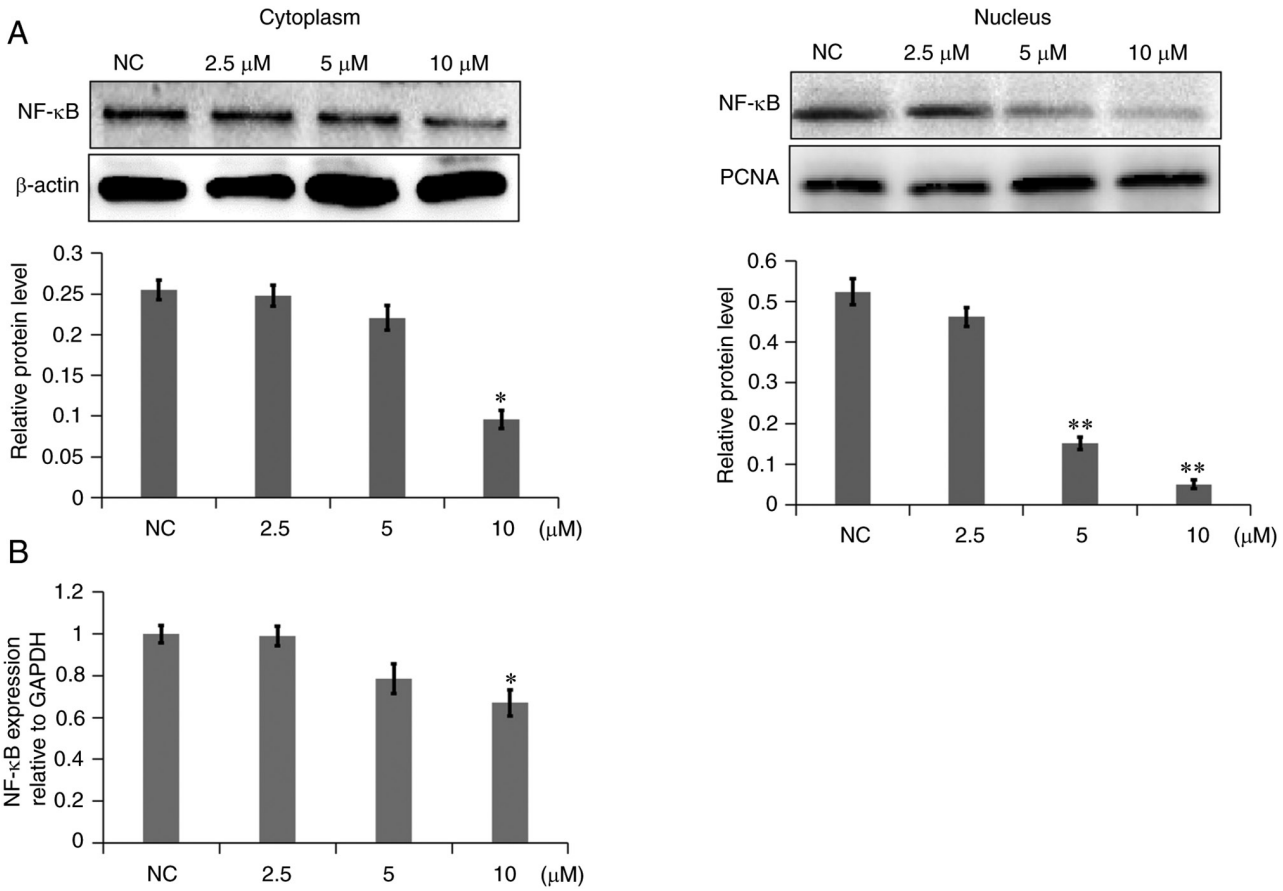

Figure 8. 7a inhibits the translocation of NF-κB into the nucleus. (A) Cytoplasmic and nuclear NF-κB was detected separately using western blot analysis. β-actin and PCNA were used as the loading controls in the cytoplasm and nucleus, respectively. (B) Expression of NF-κB mRNA transcripts normalized to GAPDH, as detected by reverse transcription-quantitative PCR. Data are presented as the mean ± SD from three separate experiments. *P<0.05 and **P<0.01 vs. NC. 7a, 2,2',4'-trihydroxychalcone; PCNA, proliferating cell nuclear antigen; NC, negative control.

decreased, as compared with those in the NC group. The gene expression levels of NF-κB were also decreased (Fig. 8B). These results demonstrated that 7a may inhibit the PI3K/AKT/NF-κB signaling pathway.

Discussion

Distant metastasis and high recurrence are the leading causes of lung cancer-related mortality (3). Traditional chemotherapy drugs become tolerated and have numerous serious adverse reactions, which have become a challenge in the treatment of lung cancer. In recent years, despite the application of various targeted drugs, the global 5-year survival rate remains very low (3,17). Therefore, more new compounds with antitumor effects and low toxicity need to be explored. Antitumor effects of certain hydroxychalcone compounds have captured the attention of several researchers. For example, studies have shown that ISL can inhibit the proliferation and induce the apoptosis of the lung adenocarcinoma cell lines A549 and NCI-H1975 (8,18). However, according to the results of previous studies, the antitumor activity of ISL is relatively weak. Therefore, more effective hydroxychalcone compounds need to be explored and understanding the antitumor mechanisms of these compounds may help identify new lung cancer treatments. The present study first aimed to investigate the antitumor effect of 7a on the biological behaviors of NSCLC cells. 7a was found to significantly inhibit the proliferation, migration, invasion and heterogeneous adhesion of A549 cells and induce cell apoptosis, indicating that 7a may have an anticancer effect on the proliferation and metastasis of A549 cells.

First, the effect of 7a on the proliferation of A549 cells was studied and it was found that 7a strongly inhibited A549 cell growth. 7a significantly inhibited migration and invasion by upregulating the expression of E-cadherin and downregulating the expression of N-cadherin in A549 cells. E-cadherin and N-cadherin are markers of epithelial-mesenchymal transition (EMT), which is a pivotal mechanism involved in the modulation of cell migration and invasion. However, in the process of EMT, the regulation of their expression occurs oppositely; E-cadherin expression is downregulated, while N-cadherin expression is often upregulated (19). The decreased expression of E-cadherin leads to the loss of E-cadherin-mediated isotype adhesion between epithelial cells, driving the high metastatic potential of tumor cells (12).

In addition, MMP-2 and MMP-9 expression was also decreased slightly in the presence of 7a. MMPs have proteolytic properties and can degrade the extracellular matrix (ECM) and participate in various biological processes, particularly tumor invasion and metastasis. During invasion and metastasis, tumor cells first bind to the basement membrane and then release MMPs, which degrade the basement membrane and ECM and finally enable tumor cells to move to the periphery along the damaged site, thus causing invasion and metastasis (20,21). Among the MMPs, MMP-2 and MMP-9 serve a crucial role in tumor invasion and metastasis. MMP-2 and MMP-9 not only degrades the matrix of cells and promotes the invasion and metastasis of tumor cells, but also participates in the occurrence and development of tumors by promoting the formation of capillaries (20,22). Thus, the present results suggested that 7a may suppress the migration and invasion of A549 cells by inhibiting the process of EMT and decreasing MMP-2/9 expression.

Heterogeneous tumor adhesion is also a pivotal step in hematogenous cancer metastasis. Cellular adhesion molecules are transmembrane proteins located on the cell membrane and the major regulators of this process, regulating cell-cell or ECM interactions. It has been reported that cell surface adhesion molecules, such as N-cadherin, CD44 and E-selectin, can promote adhesion between tumor cells and vascular endothelial cells, which eventually prevented anoikis in the blood circulation (16,23-25). In the present study, 7a was found to inhibit adhesion between A549 cells and HUVECs in a concentration-dependent manner. At the same time, N-cadherin and E-selectin expression was decreased. In addition, tumor cell angiogenesis was found to be closely associated with tumor cell invasion and metastasis. Tumor cell growth and proliferation is dysregulated and disorderly, which disrupts the previous cell balance and requires the supply of sufficient oxygen and nutrients (26). Therefore, blood vessel formation serves an essential role in tumor metastasis. In an early study, a novel tumor angiogenesis modality, VM, was first proposed to describe the ability of highly aggressive melanomas to dedifferentiate in order to acquire multiple cellular phenotypes and endothelial-like characteristics (27). This process leads to the formation of vascular-like structures of blood vessels and red blood cells, which in turn leads to angiogenesis and the insertion of a vascular-like matrix into a network of blood vessels that promotes circulation. Subsequently, several studies have reported that some malignant tumors, such as breast, ovarian and prostate cancer and NSCLC, could also form mimetic blood vessels (28-30). The present study found that 7a could inhibit the formation of VM by reducing the expression of VEGF. Specifically, in the 10 μM group, the tubular structure almost disappeared (Fig. 4). Various studies have shown that VEGF is an important pro-VM factor (14,31). VEGF is considered to promote VM by activating the PI3K/AKT signaling pathway (14).

In addition to the metastasis process, 7a could also promote A549 cell apoptosis in a concentration-dependent manner. Apoptosis, a tightly regulated process of cell death, is associated with organized stability, tumors and autoimmune and neurodegenerative diseases (32). 7a was found to reduce Bcl-2 expression while increasing Bax, cleaved PARP and caspase-3 expression. Although Bcl-2 and Bax belong to the Bcl-2 gene family, they have the opposite effect on tumor apoptosis (33). Bcl-2 inhibits the release of cytochrome c from mitochondria to the cytoplasm, thereby inhibiting apoptosis, while the overexpression of Bax can antagonize the protective effect of Bcl-2 and lead to cell death (34). Increased cytochrome c release in tumor cells can trigger the caspase cascade and PARP is then cleaved; cleaved PARP is a substrate of caspase-3 in the semicarpal protease family, eventually resulting in tumor cell apoptosis (35).

Several studies have shown that the PI3K/AKT/mTOR signaling pathway serves a crucial role in the regulation of tumor growth, apoptosis, metabolism, invasion and metastasis, as well as angiogenesis (36-38). Therefore, the regulation of this pathway has become of interest in the treatment of lung cancer. The activation of the PI3K/AKT signaling pathway can lead to the activation of several antiapoptotic proteins, such as Bcl-2, and inhibit a series of proapoptotic proteins, such as Bax, caspase and p53, thereby preventing apoptotic factors from being released from mitochondria, which inhibits tumor cell apoptosis (39). The present study found that 7a could significantly reduce the phosphorylation of key proteins of the PI3K/AKT signaling pathway, such as p-AKT, p-PI3K and

p-mTOR. As reported by Chien *et al* (40), the inhibition of the PI3K/AKT signaling pathway in cells following treatment with specific inhibitors of PI3K (such as wortmannin) could reduce the protein expression of MMP-2 and MMP-9. Another study reported that the inhibition of the PI3K/AKT/p70S6K1 signaling pathway can significantly reduce the expression of VEGF (41). NF-κB is a downstream signaling molecule in the PI3K/AKT signaling pathway and its activation is closely associated with a variety of pathologies, such as inflammation, adhesion, invasion, metastasis and angiogenesis (42). NF-κB is considered to promote the formation of EMT by upregulating E-cadherin and downregulating N-cadherin (43) and simultaneously upregulating MMP-2/9 (44). Furthermore, the inhibition of NF-κB activity by the adenovirus-mediated expression of a dominant-negative NF-κB or by the proteasome inhibitor MG132 decreases VEGF mRNA in MDA-MB-231 cells (45). NF-κB, as a multifunctional transcription factor, promotes gene transcription mainly by entering the nucleus. The present study therefore examined the NF-κB protein expression in the cytoplasm and nucleus separately. 7a treatment resulted in a marked decrease of NF-κB protein expression in the nucleus and a slight decrease in the cytoplasm. In addition, the RT-qPCR results showed that 7a also reduced the mRNA expression of NF-κB. Therefore, 7a may inhibit A549 cell activity via the PI3K/AKT/NF-κB signaling pathway.

In the present study, there was a noteworthy phenomenon; while inhibiting A549 cell migration and invasion, vasculogenic mimicry and adhesion to HUVECs, 7a might lead to apoptosis at the same concentration. How to exclude the possibility that these inhibitions of metastasis were independent of cell death? First, during the HUVEC adhesion test, most apoptotic cells were discarded after centrifugation and apoptotic cells could not be stained with DiO. The same number of viable cells was selected by cell counting and the cells were then added to a 24-well plate filled with HUVEC monolayers. So the experimental results were almost unaffected by apoptosis. During the migration, invasion and angiogenic mimicry experiments, apoptosis might have some effect, but the effect was not significant. The cell apoptosis rate was not high when the concentration of 7a was ≤5 μM for 48 h. The apoptotic rate of the 2.5 μm group was ~7.1% (the apoptosis result of this concentration was obtained but not included in Fig. 6), which was only 1.7% higher than that of the control group. The apoptosis rate of the 5 μM group was 9.6%, which was 4.2% higher than that of control group. This was much lower than the inhibition rate of 7a on migration, invasion and angiogenic mimicry. Second, the expression of related proteins also showed a trend of change, which was consistent with the experimental findings. These data indicated that 7a could indeed inhibit the A549 cell metastasis.

However, there were still some shortcomings in the present study. For example, it did not explore the molecular mechanism differences between 7a and its isomer ISL. To the best of the authors' knowledge, this was the first study to examine whether 7a had antitumor activity. So, it is not clear whether the molecular mechanisms of 7a are different from those of ISL. Thus, subsequent studies will comprise an in-depth exploration of antitumor molecular mechanisms of 7a. In addition, there were no *in vivo* experiments conducted and no use of a common antitumor drug as a control to support our observations. Therefore, further studies are required to verify the present findings.

In conclusion, the present results showed that 7a may inhibit A549 lung cancer cell proliferation and metastasis and induce apoptosis through the PI3K/AKT/NF-κB signaling pathway. Thus, 7a may be a promising flavonoid with antitumor activities that can inhibit the progression of lung cancer. Further research is required to investigate the detailed mechanism through which 7a inhibits lung cancer.

Acknowledgements

The authors acknowledge the Institute of Natural Medicinal Chemistry, Qingdao University for providing flavonoid 7a.

Funding

This work was supported by the National Natural Science Foundation of China (grant no. 81903872) and Natural Science Foundation of Shandong Province (grant no. ZR2020MH418).

Availability of data and materials

All data generated or analyzed in the present study are included in this published article.

Authors' contributions

PL conceived and designed the study. The experiments were performed by JLS, ZQC and SWS. ZHS contributed to the writing of the manuscript and designed the primers for RT-qPCR experiments. The statistical analysis was performed by SHS and JY. JLS wrote the manuscript. PL revised the manuscript. All authors have read and approved the final manuscript. JLS, ZQC and PL confirm the authenticity of all the raw data.

Ethics approval and consent to participate

The present study was approved by the Research Ethics Committee of the Affiliated Hospital of Qingdao University.

Patient consent for publication

Not applicable.

Competing interests

The authors declare that they have no competing interests.

References

1. Molina JR, Yang P, Cassivi SD, Schild SE and Adjei AA: Non-small cell lung cancer: Epidemiology, risk factors, treatment and survivorship. Mayo Clin Proc 83: 584-594, 2008.
2. Torre LA, Bray F, Siegel RL, Ferlay J, Lortet-Tieulent J and Jemal A: Global cancer statistics, 2012. CA Cancer J Clin 65: 87-108, 2015.
3. Quint LE, Tummala S, Brisson LJ, Francis IR, Krupnick AS, Kazerooni EA, Iannettoni MD, Whyte RI and Orringer MB: Distribution of distant metastases from newly diagnosed non-small cell lung cancer. Ann Thorac Surg 62: 246-250, 1996.
4. Vaya J, Belinky PA and Aviram M: Antioxidant constituents from licorice roots: Isolation, structure elucidation and antioxidative capacity toward LDL oxidation. Free Radic Biol Med 23: 302-313, 1997.

5. Chan SC, Chang YS, Wang JP, Chen SC and Kuo SC: Three new flavonoids and antiallergic, anti-inflammatory constituents from the heartwood of Dalbergia odorifera. Planta Med 64: 153-158, 1998.
6. Yamamoto S, Aizu E, Jiang H, Nakadate T, Kiyoto I, Wang JC and Kato R: The potent anti-tumor-promoting agent isoliquiritigenin. Carcinogenesis 12: 317-323, 1991.
7. Cuendet M, Guo J, Luo Y, Chen S, Oteham CP, Moon RC, van Breemen RB, Marler LE and Pezzuto JM: Cancer chemopreventive activity and metabolism of isoliquiritigenin, a compound found in licorice. Cancer Prev Res (Phila) 3: 221-232, 2010.
8. Tian T, Sun J, Wang J, Liu Y and Liu H: Isoliquiritigenin inhibits cell proliferation and migration through the PI3K/AKT signaling pathway in A549 lung cancer cells. Oncol Lett 16: 6133-6139, 2018.
9. Liang CC, Park AY and Guan JL: In vitro scratch assay: A convenient and inexpensive method for analysis of cell migration in vitro. Nat Protoc 2: 329-333, 2007.
10. Yu LG Andrews N, Zhao Q, McKean D, Williams JF, Connor LJ, Gerasimenko OV, Hilkens J, Hirabayashi J, Kasai K and Rhodes JM: Galectin-3 interaction with thomsen-friedenreich disaccharide on cancer-associated MUC1 causes increased cancer cell endothelial adhesion. J Biol Chem 282: 773-781, 2007.
11. Schmittgen TD and Livak KJ: Analyzing real-time PCR data by the comparative C(T) method. Nat Protoc 3: 1101-11108, 2008.
12. Herzig M, Savarese F, Novatchkova M, Semb H and Christofori G: Tumor progression induced by the loss of E-cadherin independent of beta-catenin/Tcf-mediated wnt signaling. Oncogene 26: 2290-2298, 2007.
13. Passalidou E, Trivella M, Singh N, Ferguson M, Hu J, Cesario A, Granone P, Nicholson AG, Goldstraw P, Ratcliffe C, *et al*: Vascular phenotype in angiogenic and non-angiogenic lung non-small cell carcinomas. Br J Cancer 86: 244-249, 2002.
14. Xu X, Zong Y, Gao Y, Sun X, Zhao H, Luo W and Jia S: VEGF induce vasculogenic mimicry of choroidal melanoma through the PI3k signal pathway. Biomed Res Int 2019: 3909102, 2019.
15. Cao Z, Hao Z, Xin M, Yu L, Wang L, Zhang Y, Zhang X and Guo X: Endogenous and exogenous galectin-3 promote the adhesion of tumor cells with low expression of MUC1 to HUVECs through upregulation of N-cadherin and CD44. Lab Invest 98: 1642-1656, 2018.
16. Xu G, Zhang W, Bertram P, Zheng XF and McLeod H: Pharmacogenomic profiling of the PI3K/PTEN-AKT-mTOR pathway in common human tumors. Int J Oncol 24: 893-900, 2004.
17. Miller KD, Siegel RL, Lin CC, Mariotto AB, Kramer JL, Rowland JH, Stein KD, Alteri R and Jemal A: Cancer treatment and survivorship statistics, 2016. CA Cancer J Clin 66: 271-289, 2016.
18. Jung SK, Lee MH, Lim DY, Kim JE, Singh P, Lee SY, Jeong CH, Lim TG, Chen H, Chi YI, *et al*: Isoliquiritigenin induces apoptosis and inhibits xenograft tumor growth of human lung cancer cells by targeting both wild type and L858R/T790M mutant EGFR. J Biol Chem 289: 35839-35848, 2014.
19. Nakajima S, Doi R, Toyoda E, Tsuji S, Wada M, Koizumi M, Tulachan SS, Ito D, Kami K, Mori T, *et al*: N-cadherin expression and epithelial-mesenchymal transition in pancreatic carcinoma. Clin Cancer Res 10: 4125-4133, 2004.
20. Merchant N, Nagaraju GP, Rajitha B, Lammata S, Jella KK, Buchwald ZS, Lakka SS and Ali AN: Matrix metalloproteinases: Their functional role in lung cancer. Carcinogenesis 38: 766-780, 2017.
21. Brown GT and Murray GI: Current mechanistic insights into the roles of matrix metalloproteinases in tumour invasion and metastasis. J Pathol 237: 273-281, 2015.
22. Thi MU, Trocmé C, Montmasson MP, Fanchon E, Toussaint B and Tracqui P: Investigating metalloproteinases MMP-2 and MMP-9 mechanosensitivity to feedback loops involved in the regulation of in vitro angiogenesis by endogenous mechanical stresses. Acta Biotheor 60: 21-40, 2012.
23. Makrilia N, Kollias A, Manolopoulos L and Syrigos K: Cell adhesion molecules: Role and clinical significance in cancer. Cancer Invest 27: 1023-1037, 2009.
24. Zhao Q, Barclay M, Hilkens J, Guo X, Barrow H, Rhodes JM and Yu LG: Interaction between circulating galectin-3 and cancer-associated MUC1 enhances tumour cell homotypic aggregation and prevents anoikis. Mol Cancer 9: 154, 2010.
25. Zhao Q, Guo X, Nash GB, Stone PC, Hilkens J, Rhodes JM and Yu LG: Circulating galectin-3 promotes metastasis by modifying MUC1 localization on cancer cell surface. Cancer Res 69: 6799-6806, 2009.
26. Popper HH: Progression and metastasis of lung cancer. Cancer Metastasis Rev 35: 75-91, 2016.
27. Maniotis AJ, Folberg R, Hess A, Seftor EA, Gardner LM, Pe'er J, Trent JM, Meltzer PS and Hendrix MJ: Vascular channel formation by human melanoma cells in vivo and in vitro: Vasculogenic mimicry. Am J Pathol 155: 739-752, 1999.
28. Shirakawa K, Tsuda H, Heike Y, Kato K, Asada R, Inomata M, Sasaki H, Kasumi F, Yoshimoto M, Iwanaga T, *et al*: Absence of endothelial cells, central necrosis and fibrosis are associated with aggressive inflammatory breast cancer. Cancer Res 61: 445-451, 2001.
29. Sood AK, Seftor EA, Fletcher MS, Gardner LM, Heidger PM, Buller RE, Seftor RE and Hendrix MJ: Molecular determinants of ovarian cancer plasticity. Am J Pathol 158: 1279-1288, 2001.
30. Sharma N, Seftor RE, Seftor EA, Gruman LM, Heidger PM Jr, Cohen MB, Lubaroff DM and Hendrix MJ: Prostatic tumor cell plasticity involves cooperative interactions of distinct phenotypic subpopulations: Role in vasculogenic mimicry. Prostate 50: 189-201, 2002.
31. Mei J, Gao Y, Zhang L, Cai X, Qian Z, Huang H and Huang W: VEGF-siRNA silencing induces apoptosis, inhibits proliferation and suppresses vasculogenic mimicry in osteosarcoma in vitro. Exp Oncol 30: 29-34, 2008.
32. Meier P, Finch A and Evan G: Apoptosis in development. Nature 407: 796-801, 2000.
33. Brown R: The bcl-2 family of proteins. Br Med Bull 53: 466-477, 1997.
34. Knight T, Luedtke D, Edwards H, Taub JW and Ge Y: A delicate balance-The BCL-2 family and its role in apoptosis, oncogenesis and cancer therapeutics. Biochem Pharmacol 162: 250-261, 2019.
35. Breckenridge DG and Xue D: Regulation of mitochondrial membrane permeabilization by BCL-2 family proteins and caspases. Curr Opin Cell Biol 16: 647-652, 2004.
36. Xia J, Dai L, Wang L and Zhu J: Ganoderic acid DM induces autophagic apoptosis in non-small cell lung cancer cells by inhibiting the PI3K/Akt/mTOR activity. Chem Biol Interact 316: 108932, 2020.
37. Zhang Z, Zhu J, Huang Y, Li W and Cheng H: MYO18B promotes hepatocellular carcinoma progression by activating PI3K/AKT/mTOR signaling pathway. Diagn Pathol 13: 85, 2018.
38. Krencz I, Sztankovics D, Danko T, Sebestyen A and Khoor A: Progression and metastasis of small cell lung carcinoma: The role of the PI3K/Akt/mTOR pathway and metabolic alterations. Cancer Metastasis Rev 27: doi: 10.1007/s10555-021-10012-4, 2021.
39. Seo BR, Min KJ, Cho IJ, Kim SC and Kwon TK: Curcumin significantly enhances dual PI3K/Akt and mTOR inhibitor NVP-BEZ235-induced apoptosis in human renal carcinoma Caki cells through down-regulation of p53-dependent Bcl-2 expression and inhibition of Mcl-1 protein stability. PLoS One 9: e95588, 2014.
40. Chien CS, Shen KH, Huang JS, Ko SC and Shih YW: Antimetastatic potential of fisetin involves inactivation of the PI3K/Akt and JNK signaling pathways with downregulation of MMP-2/9 expressions in prostate cancer PC-3 cells. Mol Cell Biochem 333: 169-180, 2010.
41. Zhong XS, Zheng JZ, Reed E and Jiang BH: SU5416 inhibited VEGF and HIF-1alpha expression through the PI3K/AKT/p70S6K1 signaling pathway. Biochem Biophys Res Commun 324: 471-480, 2004.
42. Aggarwal BB: Nuclear factor-kappaB: The enemy within. Cancer Cell 6: 203-208, 2004.
43. Zhou P, Wang C, Hu Z, Chen W, Qi W and Li A: Genistein induces apoptosis of colon cancer cells by reversal of epithelial-to-mesenchymal via a Notch1/NF-κB/slug/E-cadherin pathway. BMC Cancer 17: 813, 2017.
44. Li J, Lau GKK, Chen L, Dong SS, Lan HY, Huang XR, Li Y, Luk JM, Yuan YF and Guan XY: Interleukin 17A promotes hepatocellular carcinoma metastasis via NF-κB induced matrix metalloproteinases 2 and 9 expression. PLoS One 6: e21816, 2011.
45. Shibata A, Nagaya T, Imai T, Funahashi H, Nakao A and Seo H: Inhibition of NF-kappaB activity decreases the VEGF mRNA expression in MDA-MB-231 breast cancer cells. Breast Cancer Res Treat 73: 237-243, 2002.